16th World Conference on Earthquake Engineering, 16WCEE 2017

Santiago Chile, January 9th to 13th 2017

Paper N° 3741

Registration Code: S-N1463265697

ASSESSMENT OF SEISMIC-INDUCED POUNDING RISK BASED ON PROBABILISTIC DEMAND MODELS

E. Tubaldi[(1)], F. Freddi[(2)], M. Barbato[(3)]

(1) Research Fellow, Department of Civil Engineering, Imperial College London, UK, e.tubaldi@ic.ac.uk
(2) Research Fellow, School of Engineering, University of Warwick, UK, F.Freddi@warwick.ac.uk
(3) Associate Professor, Department of Civil & Environmental Engineering, Louisiana State University, US, mbarbato@lsu.edu

Abstract

The seismic-induced pounding between adjacent buildings is an undesirable event that can cause major damage and even structural collapse for structures with inadequate separation distance. This issue is particularly important in metropolitan areas, where the land space is limited and expensive.

In order to minimize the pounding risk, existing design codes provide simplified numerical procedures and analytical rules for estimating the minimum separation distance that is needed to avoid pounding under a target seismic hazard scenario. However, these code procedures are characterized by unknown safety levels and, thus, do not permit to control explicitly the risk of pounding or the consequences of the impact. Previous research by two of the authors developed a reliability-based design methodology for the separation distance that corresponds to a target probability of pounding during the design life of adjacent buildings. This methodology was successfully applied to linear elastic structures.

Further studies are required to make reliability-based methodologies applicable in an efficient way to more complex nonlinear building models, which require the use of computationally expensive numerical simulations to accurately predict the structural response. This paper illustrates an efficient probabilistic seismic demand model (PSDM) for pounding risk assessment consistent with modern performance-based design frameworks. A PSDM consists in the analytical representation of the relation between a seismic intensity measure (*IM*) and an engineering demand parameter (*EDP*). In this specific problem, the *EDP* of interest is the peak relative displacement between the adjacent buildings at the most likely impact location. The PSDM can be used to estimate the seismic vulnerability and the mean annual frequency of pounding between adjacent buildings via convolution with the site's hazard curve.

First, an extensive parametric study is performed by considering the case of two adjacent buildings modeled as linear single-degree-of-freedom (SDOF) systems. Different *IM*s are proposed for the problem at hand, whose choice is motivated mainly by efficiency criteria. The parametric study results are utilized to evaluate the efficiency and sufficiency of the proposed IMs employed in conjunction with a PSDM based on the linear regression of the seismic demand variation with respect to the IM in the log-log space.

Successively, the case study of two realistic steel buildings modeled as nonlinear hysteretic multi-degree-of-freedom shear-type systems is considered to evaluate the effectiveness and accuracy of the *IM*s and PSDM introduced for the buildings described as SDOF systems. A bilinear PSDM is proposed to achieve a better fit of the seismic median demand and dispersion over the entire range of seismic excitation levels. Finally, comparisons are made between the risk estimates obtained by using the linear and bilinear PSDMs and the corresponding estimates obtained via incremental dynamic analysis (IDA) in order to evaluate and compare the accuracy of the proposed regression models. It is found that the use of a bilinear PSDM in conjunction with cloud analysis provides seismic pounding risk estimates that are very close to those obtained through IDA at a small fraction of the computational cost and without scaling the records.

Keywords: Pounding, Performance-Based Design, Probabilistic Seismic Demand Model, Intensity Measure.

1. Introduction

Seismic-induced pounding between adjacent buildings is an undesirable event that can cause major damage and even structural collapse [1],[2]. This issue is particularly relevant for structures located in metropolitan areas, due to limited availability of land space. In the last three decades, extensive research was carried out to estimate the effect of pounding between adjacent structures. In most cases, the structural pounding phenomenon was shown to be detrimental to the seismic performance of adjacent buildings, by increasing accelerations and drift demands at various story levels [3],[4],[5],[6]. In order to control pounding risk, current design codes prescribe a minimum separation distance between adjacent buildings and provide simplified numerical procedures and analytical rules for estimating its value under a given seismic hazard scenario [7]. However, these code procedures are characterized by unknown safety levels and, thus, do not permit to control explicitly the risk of pounding [8],[9]. In [8], with the aim to evaluate the risk of pounding between adjacent systems, a methodology was proposed and efficiently applied to the case of buildings modeled as linear systems, for which analytical techniques can be efficiently employed to estimate with good accuracy the response statistics under the uncertain earthquake input. Based on the results presented in [8], a reliability-based methodology was proposed in [9] for the design of the separation distance between adjacent buildings for a target probability of pounding during the buildings' design life. However, despite the advancement made by these and other works, further studies are required to make these methodologies applicable to more realistic and complex nonlinear building models.

The objective of this paper is to illustrate an efficient probabilistic seismic demand model (PSDM) [10],[11],[12] for pounding risk assessment. This PSDM was previously developed by the authors [13] and is consistent with modern performance-based design frameworks such as the PEER framework [14]. A PSDM is the outcome of probabilistic seismic demand analysis (PSDA), and consists in the analytical representation of the relation between a seismic intensity measure (*IM*) and a measure of the structural response of interest, i.e., an engineering demand parameter (*EDP*). In this specific case, the *EDP* of interest is the peak relative displacement between the adjacent buildings at the most likely impact location. In the development of a PSDM, different choices can be made regarding the *IM* to be employed, the record selection, the technique used to estimate the response statistics for different *IM* levels, and the model describing the *EDP* statistics given the *IM*. In the present paper, some of these choices are discussed and evaluated by considering models of adjacent buildings with different degree of complexity.

First, the case of two adjacent buildings modeled as linear single-degree-of-freedom (SDOF) systems is considered. An extensive parametric study is performed by exploring a wide range of situations, as described by the identified non-dimensional characteristic parameters that control the system seismic behavior. The parametric study results are utilized to evaluate the efficiency and sufficiency of three different proposed *IM*s employed in conjunction with a PSDM [15],[16] and involving the linear regression of the seismic demand variation with respect to the *IM* in the log-log space. Successively, the case of two adjacent buildings described as nonlinear hysteretic multi-degree-of-freedom (MDOF) systems is analyzed, with the aim of evaluating the effectiveness and accuracy of the *IM*s and PSDM introduced for the buildings described as SDOF systems. A bilinear (in the log-log space) PSDM is also proposed to achieve a better fit of the seismic median demand and dispersion over the entire range of seismic excitation levels. Finally, comparisons are made between the risk estimates obtained by the linear and bilinear PSDMs and the corresponding estimates obtained via incremental dynamic analysis [17] in order to evaluate and compare the accuracy of the proposed regression models.

2. PSDMs for pounding risk assessment

2.1 Probabilistic seismic demand analysis

The risk of pounding between two adjacent buildings A and B, where A denotes the building providing the largest contribution to the displacement demand at the most likely impact location, can be expressed in terms of the mean annual frequency (MAF), $\nu_{EDP}(\xi)$, with which the peak relative displacement between the adjacent buildings at the most likely impact location, u_{rel} (*EDP* of interest in this problem), exceeds the separation distance ξ [8]. In this study, the most likely impact location is assumed to coincide with the roof level of the lower of the two adjacent buildings. Based on the total probability theorem, $v_{EDP}(\xi)$ is expressed as:

$$v_{EDP}(\xi) = \int_{im} G_{EDP|IM}(\xi|im) \cdot |\mathrm{d}v_{IM}(im)| \tag{1}$$

in which $G_{EDP|IM}(\xi|im)$ = complementary cumulative distribution function of $EDP = u_{rel}$ conditional to $IM = im$, and $v_{IM}(im)$ = MAF of exceedance of a specific value im. The probabilistic description of the seismic intensity measure IM through the MAF $v_{IM}(im)$ is the task of probabilistic seismic hazard analysis. The description of $G_{EDP|IM}(\xi|im)$ is the task of PSDA, and returns the PSDM, which is the object of this study. In general, the computation of $G_{EDP|IM}(\xi|im)$ involves performing a series of time-history dynamic analyses of the structural system under a set of ground-motion records with IM levels spanning the range of interest. Then, a regression analysis of the EDP samples on the corresponding IM values is carried out to obtain a synthetic probabilistic description of the seismic demand given $IM = im$ [16].

The two major issues in defining a PSDM for the problem considered in this study are related to the choice of (1) an appropriate IM, and (2) a regression model for the relation between the EDP and the IM. These two problems are strictly related, because the appropriateness of an IM is quantified by using the results of a regression analysis, and thus depends on the regression model employed.

2.2 *IM*s for pounding risk assessment

The choice of an appropriate IM is a critical issue because it affects the computational cost and the accuracy of the estimates of $G_{EDP|IM}(\xi|im)$. In general, *IM*s are selected based on efficiency, sufficiency, and hazard computability criteria [11],[12],[16]. The term 'efficiency' is related to the dispersion of the seismic demand for a given IM value [18]. The term 'sufficiency' refers to the statistical independence of the EDP with respect to typical ground motion characteristics such as magnitude (M) and source-to-site distance (R). The 'hazard computability' refers to the effort required to derive a hazard curve or attenuation law of the IM. In this paper, a regression model is fitted to the results of PSDA and the efficiency of the proposed *IM*s is measured by the degree of scatter about the regression fit. Some considerations are also made on the IM sufficiency.

In general, selecting an IM that is as close as possible to the EDP of interest is advantageous in terms of efficiency and sufficiency. Modal combination rules such as the absolute sum (ABS), square root of the sum of the squares (SRSS), and double difference combination (DDC) rules can provide approximate estimates of the relative displacement response between two adjacent systems in function of their spectral displacement [20]. The simplest IM that naturally stems from the use of spectral displacements is:

$$IM_1 = \gamma_A S_d(T_A) \tag{2}$$

where $S_d(T_A)$ denotes the spectral displacement at the fundamental period T_A and γ_A denotes the fundamental mode participation factor of building A. In computing γ_A, the modal shape is normalized to have a unit displacement at the pounding location. This intensity measure is roughly proportional to the spectral acceleration, which is widely employed in PSDA of buildings for its sufficiency and efficiency [18]. However, in the problem considered here, this IM could be not appropriate due to the potentially relevant contribution of both buildings' displacements to the peak relative displacement.

A more advanced IM can be defined as:

$$IM_2 = \gamma_A S_d(T_A)\sqrt{1+R_{BA}^2} = IM_1\sqrt{1+R_{BA}^2} \tag{3}$$

where $R_{BA} = [\gamma_B S_d(T_B)]/[\gamma_A S_d(T_A)]$. This *IM* is very similar to that proposed by [16] to reduce (when compared to using IM_1) the dispersion of buildings' inter-story drift demand by accounting also for the contribution of their second vibration mode. In the present study, IM_2 is proposed to account for the contribution to the peak relative displacement response of both systems and can be directly related to the SRSS rule for estimating the peak relative displacement.

An even more advanced *IM* can be defined as:

$$IM_3 = \gamma_A S_d(T_A)\sqrt{1+R_{BA}^2-2\rho_{BA}R_{BA}} = IM_1\sqrt{1+R_{BA}^2-2\rho_{BA}R_{BA}} \tag{4}$$

where ρ_{BA} denotes the correlation factor between the two buildings' responses [20]. This last *IM* can be directly related to the DDC rule for peak relative displacement evaluation, which is in general more accurate than the ABS and SRSS rules, especially for close fundamental vibration periods [8],[20]. A hazard curve can be easily derived for each of the proposed *IM*s when an attenuation law for $S_d(T_i)$ (i = A, B) is available [16].

The peak ground acceleration (*PGA*), referred to hereinafter as IM_0, is also considered in this work as a basic reference scalar *IM*, since it is employed in many studies for evaluating the pounding probability of buildings [8],[21].

2.3 Regression models for pounding risk assessment

Linear regression model

PSDM are often built by using the following expression as regression model between *EDP* and a scalar *IM* [15]:

$$\ln EDP|IM = \ln a + b\ln IM + \ln\varepsilon|IM \tag{5}$$

where the parameters a and b, as well as the error variable $\varepsilon|IM$ need to be estimated via regression analysis in the log-log space of the *EDP*s samples given *IM*. The variable $\varepsilon|IM$ is assumed to be lognormally distributed. Thus, the considered *EDP* follows a lognormal distribution and $\ln EDP|IM$ is normally distributed with mean value $\ln a + b\cdot\ln im$ and standard deviation $\beta_{\ln EDP|IM}(im)$. The assumed regression model permits to evaluate in closed form the complementary cumulative distribution function $G_{EDP|IM}(\xi|im)$ used in Eqn. (1) as [15]:

$$G_{EDP|IM}(\xi|im) = P[EDP|IM \geq \xi|im] = \Phi\left(\frac{\ln a + b\cdot\ln im - \ln\xi}{\beta_{\ln EDP|IM}(im)}\right) \tag{6}$$

where $\Phi(\cdot)$ denotes the standard normal cumulative distribution function. The plot of $G_{EDP|IM}(\xi|im)$ as a function of *IM* is commonly denoted as fragility curve in the literature [22].

Different techniques can be used to generate the *EDP*s samples given *IM* [15],[18],[23]. In this study, cloud analysis is employed. The use of this technique is usually coupled with the assumption of homoscedasticity of the demand, *i.e.*, the standard deviation of the *EDP* is assumed constant with respect to *IM* as $\beta_{\ln EDP|IM}(im)=\beta$ [15]. It is noteworthy that, in the case of linear elastic behavior of the two adjacent systems, b can be assumed equal to one, and the PSDM requires a simpler one parameter log-log linear regression [16]. Finally, it is worth to note that in developing the PSDM for pounding risk assessment the *EDP* samples corresponding to the earthquakes inducing building collapse should be discarded in the regression analysis.

Bilinear regression model

In some cases, the structural nonlinear behavior can strongly affect the peak relative displacement [24],[25]. In these cases, a linear relationship in the log-log plane between the *IM* and the median response could be not valid for the entire *IM* range of interest. Moreover, the nonlinear building behavior is also expected to induce an increased dispersion of the *EDP*s values, due to the reduced efficiency of an *IM* that is based on the elastic system properties. Thus, also the assumption of homoscedasticity could be not satisfied. Several alternative techniques exist to solve these issues in accurately describing the *EDP* seismic demand [10],[12]. In this paper, a bilinear PSDM [26] (see Fig. 1) is used because of its simplicity and the small number of parameters involved in the fitting. This bilinear regression model can be expressed as:

$$\ln EDP|IM = \left(a_1 + b_1 \ln IM\right) H_1 + \left(a_2 + b_2 \ln IM\right)\left(1 - H_1\right) + \ln \varepsilon|IM \tag{7}$$

in which a_i and b_i (i = 1, 2) control the intercepts and the slopes of the i-th segment, respectively (see Fig. 1), and H_1 denotes the unit step function (*i.e.*, $H_1 = 1$ for $IM \le IM^*$, and $H_1 = 0$ for $IM > IM^*$, where the parameter IM^* identifies the breakpoint, which is defined as the point of intersection of the two segments, corresponding on average to the yielding of any of the two buildings). The value of IM^* is obtained by solving the equation:

$$a_1 + b_1 \ln IM^* = a_2 + b_2 \ln IM^* \tag{8}$$

By substituting Eqn.(8) into Eqn.(7), the following alternative expression for the bilinear regression model is obtained:

$$\ln EDP|IM = \left(a_1 + b_1 \ln IM\right) H_1 + \left[a_1 + \left(b_1 - b_2\right)\ln IM^* + b_2 \ln IM\right]\left(1 - H_1\right) + \ln \varepsilon|IM \tag{9}$$

In the problem considered in this paper, the breakpoint IM^* is not known, and the model parameters $a_1, b_1, b_2, \ln IM^*$ can be estimated by performing ordinary nonlinear least square regression. The value $b_1 = 1$ can be assumed for the first segment describing the buildings' linear response. It is noteworthy that the use of a bilinear model permits to consider two different dispersions for the linear (first segment) and nonlinear (second segment) range of behavior, *i.e.*, it allows to relax the assumption of homoscedasticity.

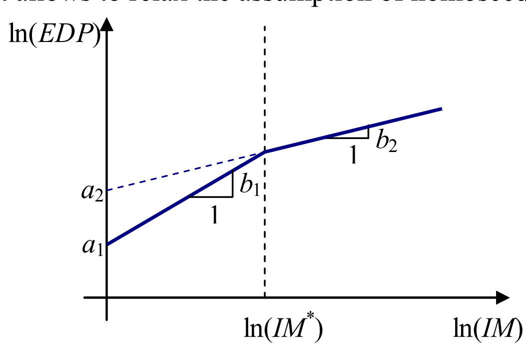

Fig. 1 – Illustration of bilinear regression model parameters.

3. Parametric study for adjacent buildings modeled as linear SDOF systems

In this section, the adjacent buildings are modeled as linear elastic SDOF systems. An extensive parametric study for a wide range of system parameters is carried out to evaluate the accuracy and efficiency of the proposed *IM*s in conjunction with the linear regression model. It is noteworthy that the use of linear elastic SDOF models for the buildings can be representative of the situations in which the buildings have a response that is dominated by their first vibration mode, are very close one to each other, and collide while vibrating in their linear range of behavior.

A dimensional analysis of the problem [27] reveals that, using an *IM* whose dimension is a length, the normalized relative displacement response between two buildings under seismic excitation can be expressed as:

$$\frac{u_{rel}}{IM_i} = f\left(T_A, \frac{T_A}{T_B}, \zeta_A, \frac{\zeta_B}{\zeta_A}\right); \quad i = 1, 2, 3 \tag{10}$$

where ζ_i (i = A, B) denotes the damping ratio corresponding to the first mode of vibration of each building. To reduce the number of parameters of the analysis, it is assumed here that $\zeta_{\mathrm{A}} = \zeta_{\mathrm{B}}$ = 2%. The vibration period T_{A} of building A is varied in the range 0-4s (with an interval of 0.2s), whereas the ratio $T_{\mathrm{B}}/T_{\mathrm{A}}$ is varied in the range 0-1 (with an interval of 0.1 up to 0.9 and of 0.025 from 0.9 to 1). The results corresponding to $T_{\mathrm{B}}/T_{\mathrm{A}}$ = 1 are obtained at the limit for $T_{\mathrm{B}}/T_{\mathrm{A}} \rightarrow 1$ from below, because IM_3 = 0 for $T_{\mathrm{B}}/T_{\mathrm{A}}$ = 1.

A set of N_{gm} = 240 records taken from [28] is selected to account for the record-to-record variability of the seismic input. Dynamic time-history analyses are carried out under the selected records and the results are fitted by using a one-parameter linear regression model obtained by assuming $b = 1$ in Eqn. (5). The parameter a_i for the i-th IM (i = 1, 2, 3) is estimated as the 50th percentile of the samples of the normalized demand u_{rel}/IM_i, whereas the dispersion β_{i} is evaluated as [16]:

$$\beta_i = \sqrt{\sum_{j=1}^{N_{gm}} \left[\ln\left(u_{rel} / IM_i\right)_j - \ln\left(a_i\right)\right]^2 / \left(N_{gm} - 2\right)}; \quad i = 1, 2, 3 \tag{11}$$

Fig. 2 reports the normalized median response a_i as a function of T_{A} and $T_{\mathrm{B}}/T_{\mathrm{A}}$, for the different IMs considered. In Fig. 2(a), which shows the results obtained by using $IM_0 = PGA$, the displacement is normalized as $u_{rel}\omega_{\mathrm{A}}^2 / IM_0$, where $\omega_{\mathrm{A}} = 2\pi/T_{\mathrm{A}}$ denotes the natural circular frequency of building A. The relative displacement demand normalized to the PGA exhibits a significant dependence on both T_{A} and $T_{\mathrm{B}}/T_{\mathrm{A}}$. It is observed that, for $T_{\mathrm{B}}/T_{\mathrm{A}}$ = 0, the values of a_0 shown in Fig. 2(a) coincide with the median pseudo spectral accelerations of the records for the vibration period T_{A}, normalized by the PGA. For the IMs based on spectral displacements (*i.e.*, IM_1, IM_2, and IM_3), the values of the normalized relative displacement demand a_i (i = 1, 2, 3) are only slightly affected by the vibration period T_{A} of building A. They slowly increase when $T_{\mathrm{B}}/T_{\mathrm{A}}$ increases from 0 to approximately 0.8 and decrease when $T_{\mathrm{B}}/T_{\mathrm{A}}$ increases from 0.8 to 1. For $T_{\mathrm{B}}/T_{\mathrm{A}} = 0 \div 0.8$ and $T_{\mathrm{A}} \geq 0.3$s, the results obtained by using IM_2 and IM_3 are only slightly biased in estimating a_i (i.e., a_i assumes values close to one for i = 2, 3), whereas those evaluated by using IM_1 are more biased, because the contribution of system B to the relative displacement response is disregarded. In the same period ranges, IM_2 practically coincides with IM_3, because the correlation factor ρ is almost zero for distant vibration periods. As $T_{\mathrm{B}}/T_{\mathrm{A}}$ approaches zero (from above), the normalized relative displacements a_i (i = 1, 2, 3) tend to slightly less than one. This phenomenon is due to the fact that the relative displacement tends to the displacement of building A, while IM_i (i = 1, 2, 3) approaches the peak absolute displacement of building A. For $T_{\mathrm{B}}/T_{\mathrm{A}}$ approaching one (from below), the normalized relative displacement response tends to zero if IM_1 or IM_2 are employed, because the two systems vibrate in phase. IM_3 is less biased in estimating the peak displacement, because it accounts for the correlation between the adjacent buildings' responses. For $T_{\mathrm{B}}/T_{\mathrm{A}}$ approaching one, IM_3 tends to zero. However, a_3 tends to a finite value which depends on the system and ground motion properties (in fact, the DDC rule and thus IM_3 provide exact estimates of the peak relative displacement only in the case of stationary response to stationary white noise excitation).

Fig. 3 reports the dispersions β_i as a function of T_{A} and the ratio $T_{\mathrm{B}}/T_{\mathrm{A}}$, for the different IMs considered. The dispersion β_0 for $IM = PGA$ assumes high values varying from about 0.50 to 1.20 (see Fig. 3(a)). As expected, β_i is significantly lower for IMs based on spectral displacements (see Fig. 3(b) through (d)). For $T_{\mathrm{B}}/T_{\mathrm{A}}$ in the range between 0 and 0.8, β_1 assumes values lower than 0.30, while β_2 and β_3 assume values lower than 0.20.

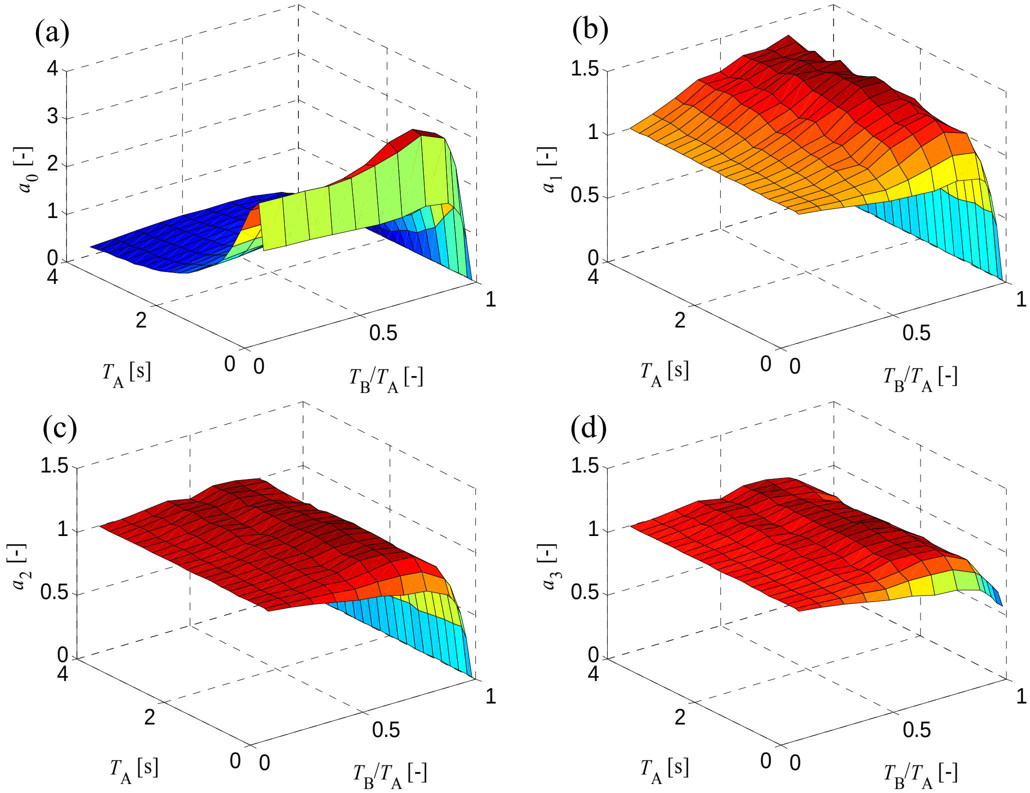

Fig. 2 – Normalized median relative displacements for different system vibration periods using as *IM*: (a) $IM_0 = PGA$, (b) IM_1, (c) IM_2, and (d) IM_3.

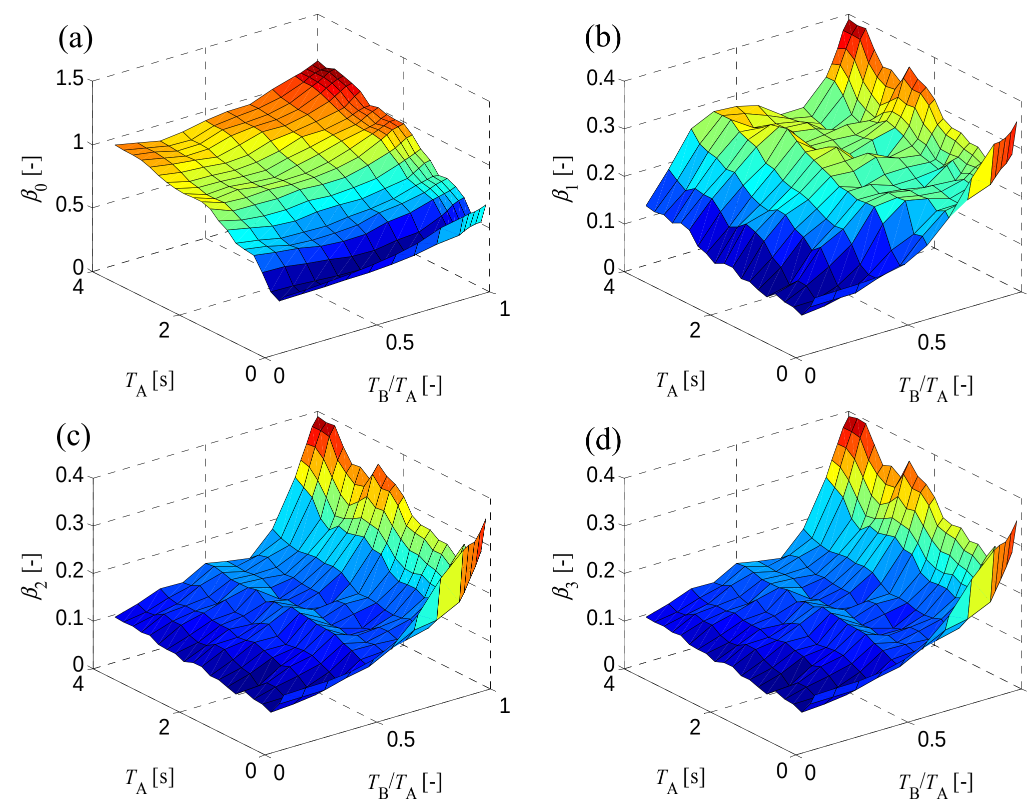

Fig. 3 – Relative displacement response dispersion β for different system vibration periods using as *IM*: (a) *PGA*, (b) IM_1, (c) IM_2, and (d) IM_3.

The higher efficiency of IM_2 and IM_3 is due to the fact that they account for the contribution of building B to the relative displacement demand. For T_B/T_A approaching one (from below), β_i increases significantly for i = 1, 2, 3, and IM_3 has an efficiency similar to that of IM_2. However, the values assumed by β_i (i = 1, 2, 3) remain lower than 0.40 in all cases considered here. An investigation of the sufficiency of the *IM*s has also been carried out but the results are not plotted here due to space constraint and the interest reader is referred to [13]. The results reveal that, while IM_0 is largely insufficient, IM_2 is sufficient for a wide range of system properties; IM_1 is more sufficient than IM_0 but less sufficient than IM_2, and IM_2 gives results comparable to IM_3.

4. Adjacent buildings modeled as nonlinear hysteretic MDOF systems

4.1 Case study description

In this section, PSDA is applied to evaluate the PSDM for the case study of two adjacent steel moment-resisting frame buildings with nonlinear hysteretic behavior. The same buildings already analyzed in [9] are considered here (Fig. 4). Building A is an eight-story shear-type building with constant inter-story stiffness k_A = 628,801kN/m and floor mass m_A = 454,550kg, while building B is a four-story shear-type building with constant inter-story stiffness k_B = 470,840kN/m and floor mass m_B = 454,550kg. The story heights are equal to 3.2m for both buildings. A Rayleigh-type damping matrix is used to model the inherent viscous damping in the two systems. The matrix is built by assigning a damping ratio ζ_R = 2% to the first two vibration modes of each system considered independently from the other. The fundamental vibration periods of the two buildings are T_A = 0.915s and T_B = 0.562s, respectively. A bilinear hysteretic constitutive model with kinematic hardening describes the relationship between the inelastic inter-story restoring force and inter-story drift [24]. This constitutive model for building i (with i = A, B) is defined by the yield force, $F_{y,i}$, and by the ratio of the post-yield to initial stiffness, r_i, which is assumed equal to 0.05 for both models. The inter-story yield forces for system A and B are respectively $F_{y,A}$ = 6,871.4kN and $F_{y,B}$ = 3,755.4kN and are derived from [21]. The participation factors for the first vibration modes of the two buildings are: γ_A = 0.855 and γ_B = 1.241.

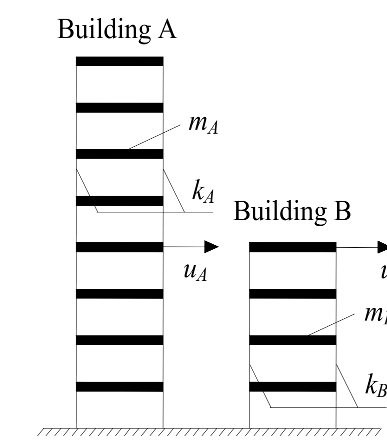

Fig. 4 – Models of buildings A and B.

4.2 Linear and bilinear PSDMs

Cloud analysis is applied here by employing the same set of 240 records already considered in the previous section. Since the buildings are expected to undergo significant inelastic deformations for a large number of records, the *EDP* samples corresponding to values of the peak inter-story drift (IDR) demand for the systems higher than 4% are discarded in developing the PSDM. The 4% limit is taken from FEMA 356 [29] and corresponds to the collapse limit states for steel moment-resisting frame buildings. A reduced set of samples (consisting of 234 out of 240 relative displacement responses conditioned on not exceeding the IDR limit of 4%) is used to derive the PSDMs conditioned on no collapse for this application example.

Two sets of linear and bilinear PSDMs are developed for each of the four *IM*s considered in the previous section. It is found that $IM_0 = PGA$ provides very high relative displacement demand dispersions (close to 0.45 for both linear and bilinear PSDM), whereas the results obtained using IM_2 and IM_3 are practically identical, given that the correlation coefficient ρ_{BA} assumes a very low value, *i.e.*, 0.0064. Thus, only the results obtained for IM_1 and IM_2 are shown and commented hereinafter. Fig. 5(a) and (b) report the response samples and the fitted median demand obtained by using the linear and bilinear PSDMs for IM_1 and IM_2, respectively. For the linear PSDMs, the values of the regression parameter b assume values contained between 0.6 and 0.7.

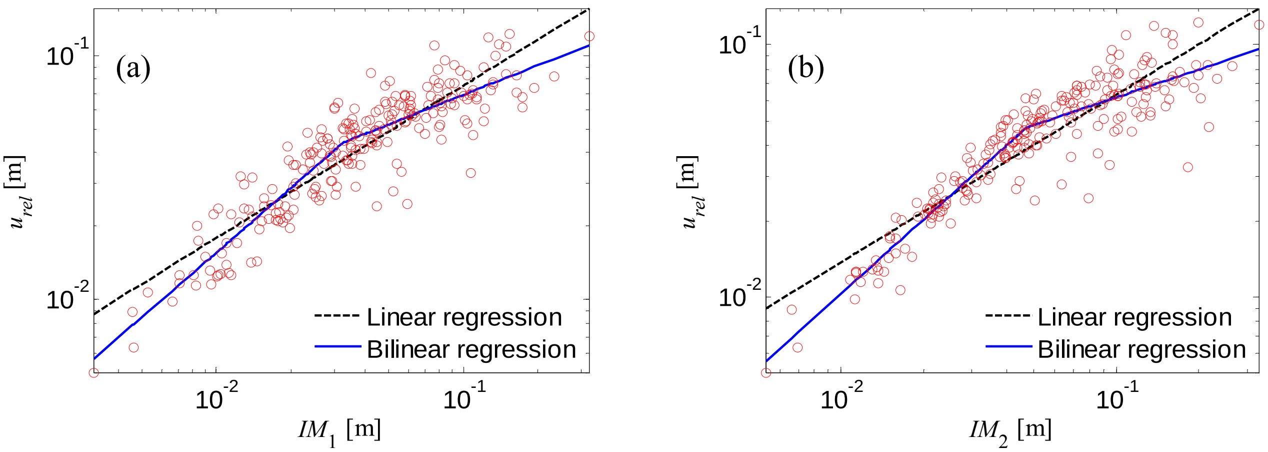

Fig. 5 – Comparison of linear and bilinear regression PSDMs in the log-log plane by using as *IM*: (a) IM_1, and (b) IM_2.

The bilinear regression model offer the possibility to overcome the assumption of homoscedasticity by defining two values for the dispersion respectively for 'low' and 'high' *IM* values. This regression model provides better results in terms of efficiency than the linear model. In fact, in the bilinear case the values of the dispersion respectively for 'low' and 'high' *IM* values are equal to 0.231 and 0.236 in the case of IM_1 (against 0.262 of the linear case) and 0.146 and 0.248 in the case of IM_2 (against 0. 250 of the linear case). These values of the dispersion confirm the superiority of IM_2 in terms of efficiency in the case of linear structural behavior, consistently with the results reported in the previous section for the SDOF linear models.

4.2 Comparison of linear and bilinear PSDMs for seismic risk assessment

In this section, the results of a seismic risk assessment analysis obtained using the linear and bilinear PSDMs developed in the previous section are compared. The fitted linear and bilinear PSDMs are employed to estimate via Eq. (6) the probability of pounding conditioned on no collapse for different values of the separation distance ξ in the range between 0m and 0.2m and for different values of the employed *IM*s. Fig. 6 shows the fragility curves obtained using IM_2 for $\xi = 0.05$m (Fig. 6(a)) and $\xi = 0.09$m (Fig. 6(b)).

Fig. 6 also shows the numerical fragility curves obtained through incremental dynamic analysis (IDA) [17]. These curves are obtained by scaling all the 240 records to discrete common *IM* values and directly comparing the response samples to the capacity (*i.e.*, the separation distance). The numerical fragility curves obtained via cloud analysis by employing a bilinear PSDM are close to the corresponding curves estimated using IDA and are derived at only a small fraction of the computational cost of the corresponding IDA-based curves.

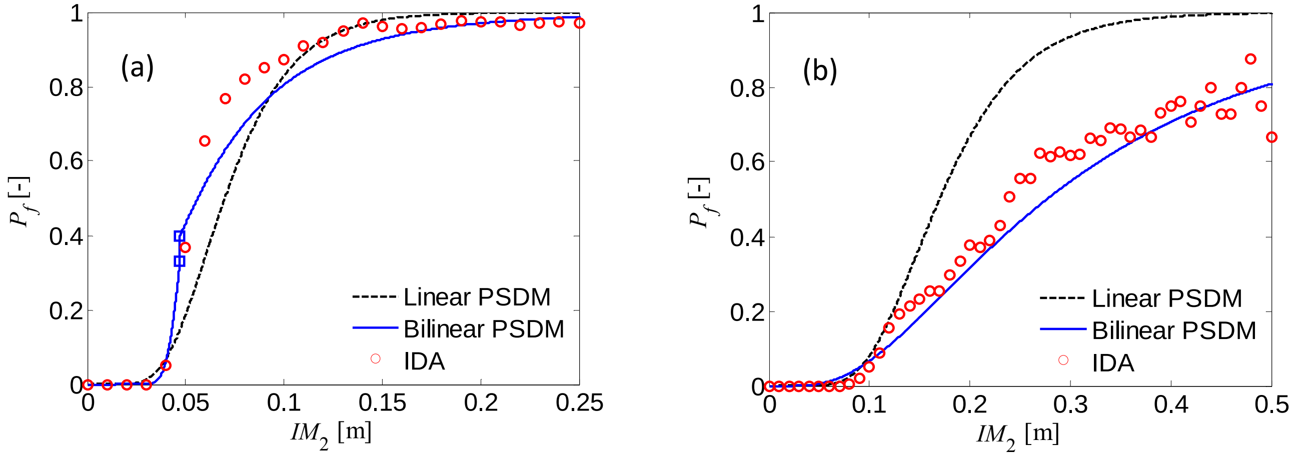

Fig. 6 – Fragility curves obtained by linear PSDM, bilinear PSDM, and IDA for IM_2 and different values of the separation distance: (a) ξ = 0.05m and (b) ξ = 0.09m.

The MAF of pounding for a given deterministic separation distance ξ, $v_f = v_{EDP}(\xi)$, is also evaluated through the procedure reported in [8] by assuming that the buildings are located in Los Angeles, CA. The information on the seismic hazard curve for the site is taken from the United States Geological Survey's (USGS) website, which provides the MAF of exceedance for the PGA and spectral accelerations at discrete periods in the range between 0.1s and 4.0s. The MAFs of exceedance of the proposed IMs, $v_{IM}(im)$, are obtained by interpolating the available hazard curves. Fig. 7(a) reports the hazard curve $v_{IM}(im)$ for IM_1 and IM_2, whereas Fig. 7(b) shows the MAF of pounding for ξ in the range between 0m and 0.3m obtained for IM_2 through the linear PSDM, bilinear PSDM, and IDA.

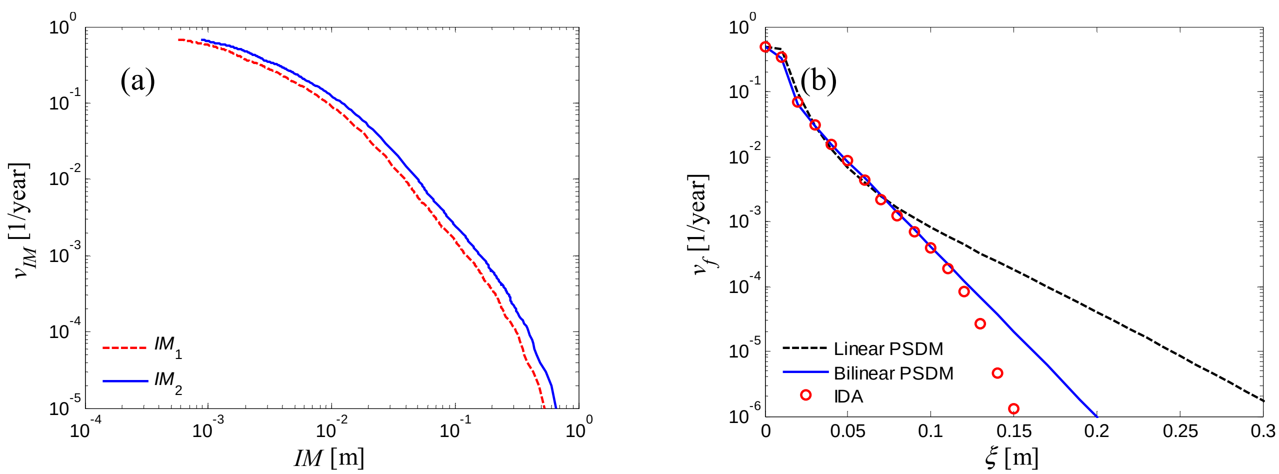

Fig. 7 – Seismic risk analysis: (a) hazard curve for IM_1 and IM_2 at the selected location (Los Angeles, CA), and (b) MAF of pounding based on IM_2 for different values of the separation distance and estimated using linear PSDM, bilinear PSDM, and IDA.

The three techniques provide very similar results for separation distances between 0m and 0.07m. For ξ values higher than 0.07m, the results obtained using cloud analysis in conjunction with the bilinear regression model are close to the results obtained through IDA, whereas the linear model provides highly conservative estimates of the pounding risk. Similar results are obtained by using IM_1 and, thus, are not reported here due to space constraints.

5. Conclusions

This paper presents an efficient and accurate probabilistic seismic demand model (PSDM) for assessing the risk of pounding between adjacent buildings within modern Performance-Based Earthquake Engineering (PBEE) frameworks. The model is defined by using different advanced intensity measures, based on well-known design rules for estimating the buildings' separation distance, and a bilinear regression model for the response samples obtained by cloud analysis.

An extensive parametric study is carried out for adjacent buildings modeled as single-degree-of-freedom linear systems under a suite of 240 natural ground motion records. The parametric study results reveal that intensity measures (*IM*) based on rules for separation distance design, such as the square root of the sum of the squares (IM_2) and the double difference combination (IM_3) rules, are superior in terms of efficiency to more common *IM*, *i.e.*, to $IM_0 = PGA$, and to the spectral displacement at the fundamental period of the taller building (IM_1).

A case study of two realistic steel buildings modeled as nonlinear hysteretic multi-degree-of-freedom shear-type systems is also analyzed in detail. Linear and bilinear PSDMs are considered to describe the relative displacement demand at the most likely pounding location. Based on the results of the study, the following conclusions are drawn: (1) IM_2 and IM_3 are more efficient intensity measures than *PGA* and IM_1, even when inelastic seismic behavior is taken into account; (2) the *IM* efficiency is higher while using the bilinear PSDM than the linear PSDM, at least in the linear behavior range; (3) the bilinear PSDM provides a more accurate description of the seismic demand than the linear PSDM, since it is able to account for the changes of the relative displacement demand (in terms of median value and dispersion) due to structural yielding; and (4) the use of a bilinear PSDM in conjunction with cloud analysis provides seismic pounding risk estimates that are very close to those obtained through incremental dynamic analysis at a small fraction of the computational cost and without scaling the records. Thus, the bilinear PSDM in conjunction with cloud analysis is recommended for seismic pounding risk analysis of buildings with nonlinear structural behavior.

6. Acknowledgments

The third author gratefully acknowledges partial support of this research by the Louisiana Department of Wildlife and Fisheries through award #724534 and the National Science Foundation (NSF) through award CMMI #1537078. Any opinions, findings, conclusions, or recommendations expressed in this paper are those of the authors and do not necessarily reflect the views of the sponsors.

7. References

[1] Anagnostopoulos SA (1988): Pounding of buildings in series during earthquakes. *Earthquake Engineering & Structural Dynamics*, **16**(3), 443-456.

[2] Cole GL, Dhakal RP, Turner FM (2012): Building pounding damage observed in the 2011 Christchurch earthquake. *Earthquake Engineering & Structural Dynamics*, **41**(5), 893–913.

[3] Papadrakakis M, Mouzakis HP (1995): Earthquake simulator testing of pounding between adjacent buildings. *Earthquake Engineering & Structural Dynamics*, **24**(6), 811–834.

[4] Polycarpou PC, Komodromos P (2010): Earthquake-induced poundings of a seismically isolated building with adjacent structures. *Engineering Structures*, **32**(7), 1937-1951.

[5] Jankowski R (2005): Non-linear viscoelastic modelling of earthquake-induced structural pounding. E*arthquake Engineering & Structural Dynamics,* **34**(6), 595-611.

[6] Efraimiadou S, Hatzigeorgiou GD, Beskos DE (2013): Structural pounding between adjacent buildings subjected to strong ground motions. Part I: The effect of different structures arrangement. *Earthquake Engineering & Structural Dynamics*, **42**(10), 1509-1528.

[7] European Committee for Standardization (ECS) (2005): *Eurocode 8 - Design of structures for earthquake resistance* (EN1998), Brussels, Belgium.

[8] Tubaldi E, Barbato M, Ghazizadeh SA (2012): Probabilistic performance-based risk assessment approach for seismic pounding with efficient application to linear systems. *Structural Safety*, **36–37**: 14–22.

[9] Barbato M, Tubaldi E (2013): A probabilistic performance-based approach for mitigating the seismic pounding risk between adjacent buildings. *Earthquake Engineering & Structural Dynamics*, **42**(8): 1203–1219.

[10] Aslani H, Miranda E (2005): Probability-based seismic response analysis. *Engineering Structures*, **27**(8), 1151-1163.

[11] Padgett JE, Nielson BG, DesRoches R (2008): Selection of optimal intensity measures in probabilistic seismic demand models of highway bridge portfolios. *Earthquake Engineering & Structural Dynamics*, **37**(5): 711–725.

[12] Rajeev P, Franchin P and Tesfamariam S (2014): Probabilistic Seismic Demand Model for RC Frame Buildings Using Cloud Analysis and Incremental Dynamic Analysis. *10th National Conference on Earthquake Engineering*, Anchorage, Alaska.

[13] Tubaldi E, Freddi F, Barbato M (2016): Probabilistic seismic demand model for pounding risk assessment. *Earthquake Engineering & Structural Dynamics*. DOI: 10.1002/eqe.2725.

[14] Zhang Y, Acero G, Conte J, Yang Z, Elgamal A (2004): Seismic reliability assessment of a bridge ground system. *13th World Conference on Earthquake Engineering*, Vancouver, Canada.

[15] Cornell CA, Jalayer F, Hamburger RO, Foutch DA (2002): Probabilistic Basis for 2000 SAC Federal Emergency Management Agency Steel Moment Frame Guidelines. *Journal of Structural Engineering*, **128**(4), 526-533.

[16] Luco N, Cornell CA (2007): Structure-specific scalar intensity measures for near-source and ordinary earthquake ground motions. *Earthquake Spectra*, **23**(2), 357-92.

[17] Vamvatsikos D, Cornell CA (2002): Incremental dynamic analysis. *Earthquake Engineering & Structural Dynamics*, **31**(3), 491–514.

[18] Shome N, Cornell CA (1999): Probabilistic seismic demand analysis of nonlinear structures. Reliability of Marine Structures, *Report No. RMS-35*. Department of Civil and Environmental Engineering, Stanford University, California.

[19] Vega J, Del Rey I, Alarcon E (2009): Pounding force assessment in performance-based design of bridges. *Earthquake Engineering & Structural Dynamics*, **38**(13), 1525–1544.

[20] Lopez-Garcia D, Soong TT (2009): Assessment of the separation necessary to prevent seismic pounding between linear structural systems. *Probabilistic Engineering Mechanics*, **24**(2), 210-223.

[21] Lin JH (2005): Evaluation of seismic pounding risk of buildings in Taiwan. *Chinese Institute of Engineers*, **28**(5), 867-872.

[22] Mackie KR, Stojadinovic B (2004): Fragility Curves for Reinforced Concrete Highway Overpass Bridges. *13th World Conference on Earthquake Engineering*, Vancouver, BC.

[23] Baker JW (2007): Probabilistic structural response assessment using vector-valued intensity measures. *Earthquake Engineering & Structural Dynamics*, **36**(13), 1861–1883.

[24] Lopez-Garcia D, Soong TT (2009): Evaluation of current criteria in predicting the separation necessary to prevent seismic pounding between nonlinear hysteretic structural systems. *Engineering Structures*, **31**(5), 1217-1229.

[25] Tubaldi E, Barbato M (2015): DISCUSSION: Probabilistic risk analysis of structural impact in seismic events for linear and nonlinear systems. *Earthquake Engineering & Structural Dynamics*, **44**(3), 491–493.

[26] Bai JW, Gardoni P, Hueste MBD (2011): Story-specific demand models and seismic fragility estimates for multi-story buildings. *Structural Safety*, **33**(1), 96-107.

[27] Barenblatt GI (1987): *Dimensional Analysis*, Gordon and Breach Science Publishers, New York.

[28] Baker JW, Jayaram N, Shahi S (2011): *Ground Motion Studies for Transportation Systems*. PEER Website.

[29] Federal Emergency Management Agency (2000): *FEMA 356: Prestandard and Commentary for the Seismic Rehabilitation of Buildings*. Washington DC.